AD_____

Award Number: W81XWH-04-1-0034

TITLE: Enhanced Ultrasound Visualization of Bracytherapy Seeds by a Novel Magnetically Induced Motion Imaging Method

PRINCIPAL INVESTIGATOR: Stephen McAleavey, Ph.D.

CONTRACTING ORGANIZATION: University of Rochester
Rochester, NY 14627

REPORT DATE: April 2008

TYPE OF REPORT: Annual

PREPARED FOR: U.S. Army Medical Research and Materiel Command
Fort Detrick, Maryland 21702-5012

REPORT DOCUMENTATION PAGE

Form Approved
OMB No. 0704-0188

1. REPORT DATE	2. REPORT TYPE	3. DATES COVERED
01-04-2008	Annual	1 Apr 2007 – 31 Mar 2008

4. TITLE AND SUBTITLE

Enhanced Ultrasound Visualization of Bracytherapy Seeds by a Novel Magnetically Induced Motion Imaging Method

5a. CONTRACT NUMBER

5b. GRANT NUMBER
W81XWH-04-1-0034

5c. PROGRAM ELEMENT NUMBER

6. AUTHOR(S)

Stephen McAleavey, Ph.D.

E-Mail: stephenm@bme.rochester.edu

5d. PROJECT NUMBER

5e. TASK NUMBER

5f. WORK UNIT NUMBER

7. PERFORMING ORGANIZATION NAME(S) AND ADDRESS(ES)

University of Rochester
Rochester, NY 14627

8. PERFORMING ORGANIZATION REPORT NUMBER

9. SPONSORING / MONITORING AGENCY NAME(S) AND ADDRESS(ES)
U.S. Army Medical Research and Materiel Command
Fort Detrick, Maryland 21702-5012

10. SPONSOR/MONITOR'S ACRONYM(S)

11. SPONSOR/MONITOR'S REPORT NUMBER(S)

12. DISTRIBUTION / AVAILABILITY STATEMENT
Approved for Public Release; Distribution Unlimited

13. SUPPLEMENTARY NOTES

14. ABSTRACT

We report our progress in developing Magnetically Induced Motion Imaging (MIMI) for unambiguous identification and localization brachytherapy seeds in ultrasound images. Coupled finite element and ultrasound imaging simulations have been performed to demonstrate that seeds are detectable with MIMI regardless of orientation to the imaging transducer and even when the seed itself is invisible in B-scans. in-vitro scans of a seed parallel and perpendicular to the transducer corroborate the simulation results.

15. SUBJECT TERMS
Prostate Cancer

16. SECURITY CLASSIFICATION OF:			17. LIMITATION OF ABSTRACT	18. NUMBER OF PAGES	19a. NAME OF RESPONSIBLE PERSON
a. REPORT	b. ABSTRACT	c. THIS PAGE			USAMRMC
U	U	U	UU	12	19b. TELEPHONE NUMBER *(include area code)*

Table of Contents

Introduction

We have devised a method called Magnetically Induced Motion Imaging (MIMI) for identifying brachytherapy seeds in ultrasound images. Ultrasound guided brachytherapy [Holm1983, Nag1997] is a common treatment for prostate cancer. The overall goal of this project is the unambiguous identification and accurate localization of brachytherapy seeds with ultrasound. Accurate determination of seed location is critical in delivering the correct dose distribution to the prostate. Automatic seed segmentation and real-time dose planning are enabled by this technique. Furthermore, the technique enables ultrasound to replace CT for post-implant evaluation, by providing a mechanism by which implanted seeds may be reliably identified by ultrasound. The proposed research will investigate and optimize the materials, instrumentation and algorithms for MIMI, to develop simulation, analytic and phantom methods to explore the relevant phenomena, and to conduct clinically realistic evaluations of the method.

Body

This report documents activities related to this grant for the period of April 1 2007 to March 30 2008. The grant was originally awarded to the PI April 1 2004 at Duke University. The work was suspended the following month when the PI transferred to the University of Rochester. Work resumed at Rochester June 2005. The PI applied for and was granted a no-cost extension to cover the interruption in work so all tasks may be completed.

The Statement of Work identifies the following tasks:

Task 1. Modeling of seed electromechanics (Months 1-18)

- A) Propose magnetic core geometry
- B) Develop finite-element model of magnetic seed core for electromagnetic simulation
- C) Solve for seed forces as a function of field strength, orientation and gradient
- D) Iteratively modify core design to maximize induced force given a constant-volume constraint

Task 2. Modeling of seed-tissue mechanics (Months 6-24)

- A) Develop finite-element mesh of seed and tissue
- B) Solve for steady-state vibration amplitude over 50-500Hz band
- C) Calculate vibration amplitude of seed vs. frequency
- D) Find iso-amplitude contours within tissue as a function of vibration frequency

Task 3. Seed detection algorithm development (Months 12-36)

- A) Simulate ultrasound RF echoes from seed and tissue vibrating as determined in Task 2 for varying seed-beam angle
- B) Evaluate motion detection and clutter suppression methods
- C) Determine vibration frequency which provides maximum spatial resolution

Task 4. In-vitro implementation (12-36)

- A) Fabricate or procure model seeds based on core design developed in Task 1
- B) Procure prostate phantom
- C) Implant seeds and clutter targets in prostate phantom
- D) Capture RF echo data and generate seed images using the algorithm of Task 3
- E) Implant seeds in excised animal tissue samples and image using the algorithm of Task 3

Here we describe our progress with regard to these tasks since the last annual report. The majority of the work has focused on tasks 3 and 4. Tasks 1 and 2 are substantially complete as scheduled.

Task 1: Seed electromechanical force modeling

Task 1 is substantially complete, as per the proposed schedule. We have determined through finite element simulations [McAleavey] that a cylinder of length equal to the length of the seed provides nearly (within 10%) the maximum torque of all shapes in response to an applied magnetic field. For the purposes of the proposed research the increase in torque achieved by the optimal shape (an end-weighted configuration) is not commensurate with the increased effort required to machine the core. The slight reduction in torque is not expected to alter the results of later tasks.

Task 2: Modeling of seed-tissue mechanics

No new simulations of seed-tissue mechanics were carried out during the period of this report, and this task is complete.

Tasks 3: Seed detection algorithm development

In this period we have carried out simulations and preliminary in vitro scans of seeds over a range of orientations to contrast B-mode performance with MIMI performance in imaging seeds.

Simulations were conducted both of seeds imaged with the seed's major axis in the scan plane. The simulations were performed using Field II [Jensen]. These simulations do not include seed reverberation effects, but do accurately model the change in backscatter as a function of seed/beam angle. Seeds were modeled as a dense (~1/2 λ between scatterers) collection of point scatterers, while the background was modeled as a diffuse collection of randomly distributed point scatterers. The same arrangement of scatterers was used for each simulation, with the entire collection of scatterers rotated through an angle of 0-90 degrees.

The simulated seed was scanned from 0 to 90 degrees (parallel to perpendicular to the transducer face) in 10 degree increments. The resulting scans are shown in figure 1. As expected, the echo from the seed decreases rapidly as its angle to the transducer increases. For angles of greater than 20 degrees the seed is difficult to detect, and for angles greater than 30 the seed is invisible in B-mode images. These images simulate a seed in a homogenous speckle environment. In the presence of other structures (calcification, air bubbles due to needle insertions) one would expect even greater difficulty in distinguishing seeds. Later simulations will include modeling of Echoseed^{TM} type seeds, which offer improved B-mode imaging away from normal incidence.

Simulations of MIMI imaging of seeds was performed through a combination of finite element simulation of seed/tissue motion and ultrasound scattering simulation. Comsol Multiphysics [Comsol] was used to simulate motion of a seed embedded in tissue. Tissue was modeled as a linear elastic material with a shear modulus of 10kPa and density of 1000kg/m^3. The seed was modeled as a 5mm long, 1mm diameter solid steel cylinder. A sinusoidally varying torque of 200Hz frequency was applied to the seed, and the transient solution calculated until a steady state was achieved. A custom Matlab code was developed to translate displacements of the seed and tissue to the ultrasound scatterers used in the Field II described previously. All motion within the scan plane (lateral and axial) was applied. Displacement amplitude was scaled to a maximum of 0.5 λ at the seed ends. The seed and tissue were imaged with the seed at 0, 10, 20, 30, and 90 degrees to the transducer face. The scatterers were displaced and scanned at 11 time steps within a single cycle of steady-state oscillation to simulate Doppler scanning with a 20kHz PRF. The motion of the seed and tissue was tracked by windowed cross-correlation [Palmeri], with a window length of 2.5 μs (12.5 λ).

Images of estimated displacement amplitude from the RF echo sequence are shown in figure 2 for 0-90 degree scan angles. As can be seen from the figures, the seed remains visible over the entire range of angles, in contrast to the B-mode images of the seed. Figure 3 shows the same images presented with a larger dynamic range, showing that it is possible to more precisely localize the seed ends over a range of angles. These simulations confirm our hypothesis that seeds remain visible in MIMI images, even when the seed is invisible in the corresponding B-mode image, due to the induced motion of the surrounding tissue. Tissue has an omni-directional scattering characteristic. The Doppler signal (echo displacement signal) imposed on the tissue by seed motion can thus be detected even when the seed itself is not visible.

In vitro imaging of a seed in a tissue-mimicking phantom was also performed in this period. Figure 4 shows images of a seed at 0 and 90 degrees to the transducer face. The power Doppler signal due to the seed is visible in both orientations, while the seed itself is invisible B-mode at the 90 degree orientation. Scans were performed for applied magnetic field frequencies of 100/150Hz, 500Hz, and 1000Hz. Increasing the drive frequency results in a more localized Doppler signal. While this is due in part to the reduce magnetic field developed at high frequency due to coil inductance, the higher

frequency shear waves induced are also damped more rapidly by the tissue-like material, resulting in a more tightly localized seed. Both low and high frequency seed drive are useful – low frequency for finding misplaced seeds, and high frequency for precise localization of a seed of known position.

We have also developed a method for detecting and compensating for physiological tissue motion and transducer movement, i.e. motion not due to seed vibration. Such compensation is necessary, as motion not related to seed vibration will produce a Doppler clutter signal that could potentially obscure seeds. This method relies on the fact that physiological and transducer motion is relatively slow and induces a low frequency Doppler signal, on the order of 10's of Hz. In contrast, the seed vibration is controllable and typically on the order of 100's of Hz to a few kilohertz.

In our clutter suppression method, illustrated schematically in figure 5, we estimate the low frequency component of tissue motion. This low-frequency component is illustrated in figure 5a, where a slow gross motion away from the transducer results in a given echo arriving progressively later after pulse transmission. This gross motion is estimated using standard Doppler [Kasai] methods and fit to a constant velocity. A "motion-compensated" Doppler ensemble is then formed by time shifting each echo by the amount estimated. The remaining Doppler ensemble contains only signal due to seed vibration, or high-frequency noise. This method has produced >10db suppression of Doppler clutter in our measurements.

Task 4:
We have designed seeds based on our results in Task 1. We have ordered a several prostate-mimicking phantoms (CIRS, Inc.) designed for simulation of seed implantation. We will be imaging these phantoms with our technique in the next few months.

Key research accomplishments in this period:

- Finite-element model of seed-tissue motion
- Ultrasound simulation of seed and tissue echo for static B-mode imaging
- Simulation of ultrasound imaging of vibrating seed, using finite element calculated scatterer displacements
- Displacement amplitude images showing MIMI sensitivity to all seed orientations, even when seed is invisible in B-scan images
- In-vitro scans corroborating simulation results

Reportable Outcomes:

Publications:

1. Stephen A. McAleavey, Thomas B. Jones, Nicholas G. Green, "Shape Optimization of Elongated Particles for Maximum Electrical Torque," *Proceedings of Electrostatics 2007*, to appear

Conclusions:

This report has described the work performed from April 2007 to March 2008. Task 1 is essentially complete, with a cylindrical shape being chosen for the seed's magnetic core as a compromise between torque maximization and manufacturing complexity. Significant progress was made in Tasks 1 and 3. The important simulation result is the demonstration that seeds are detectable in MIMI images regardless of orientation. We have demonstrated in vitro a clutter-suppression method to compensate for tissue and transducer motion. This method prevents physiological or transducer scanning motion from obscuring the Doppler signal generated by seed vibration.

References:

[Comsol2004] *Electromagnetics Module User's Guide*, Comsol AB, 2004

[Jensen] [1] J.A. Jensen, "Field: A Program for Simulating Ultrasound Systems," *10th Nordic-Baltic Conference on Biomedical Imaging Published in Medical & Biological Engineering & Computing*, pp. 351-353, Volume 34, Supplement 1, Part 1, 1996.

[Kasai] C. Kasai et al., "Real-Time Two-Dimensional Doppler Flow Mapping Using Auto-Correlation," *Acoustical Imaging: Proceedings of the International Symposium,* v 13, 1984, p 447-460

[McAleavey] S.A. McAleavey, T.B. Jones, N.G. Green, "Shape Optimization of Elongated Particles for Maximum Electrical Torque," *Proceedings of Electrostatics 2007*, to appear

[Palmeri] M.L. Palmeri, S.A McAleavey, G.E. Trahey, K.R. Nightingale, "Ultrasonic tracking of acoustic radiation force-induced displacements in homogeneous media," *IEEE Transactions on Ultrasonics Ferroelectrics and Frequency Control*. 2006 Jul;53(7):1300-13.

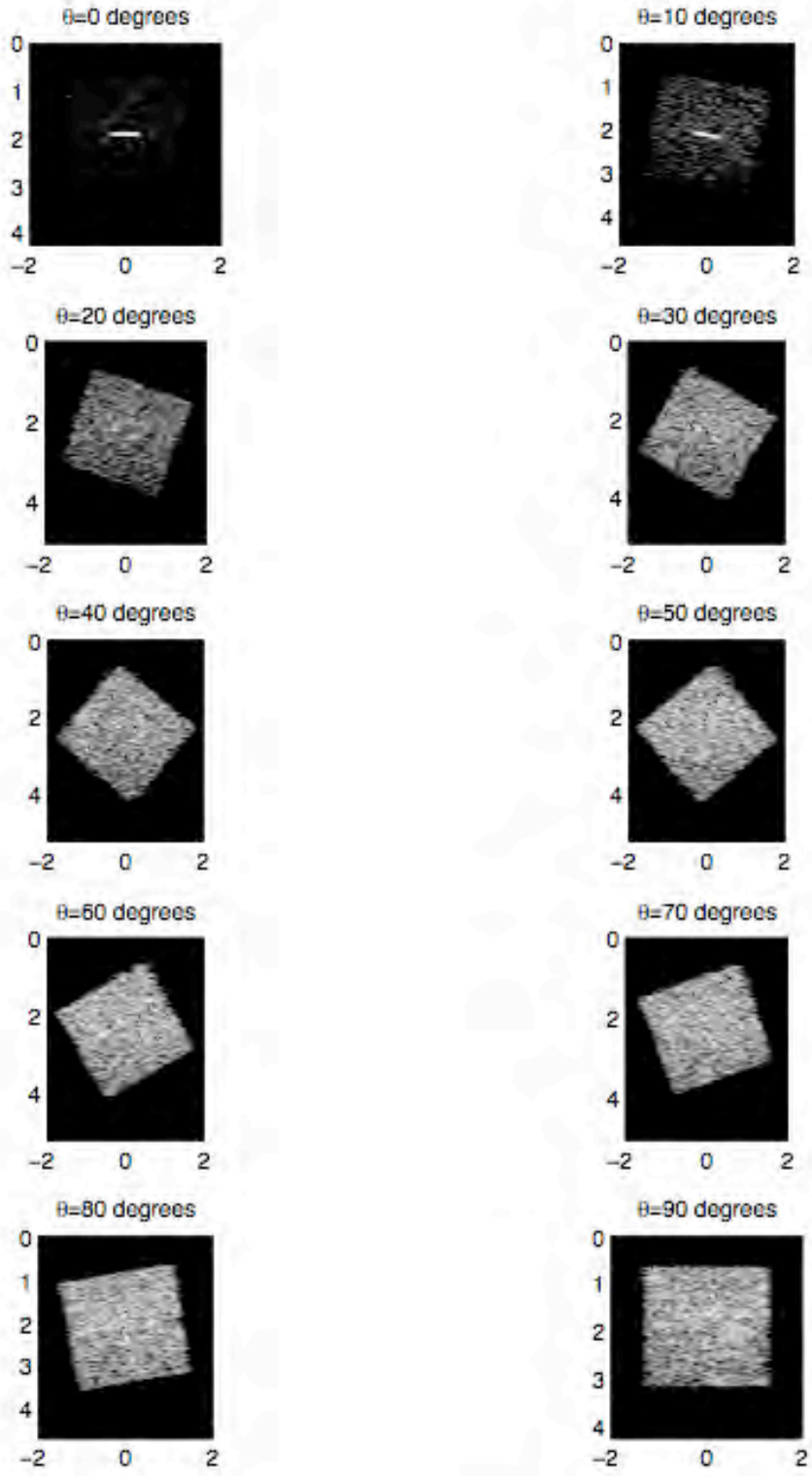

Figure 1. Simulated B- mode images of seeds at 0-90 degrees to the transducer face. Note that the seed is significantly obscured at 20 degrees, and invisible for angles of greater than 30 degrees. The system simulated is a 128 channel, 5MHz linear array with apodization and dynamic focusing

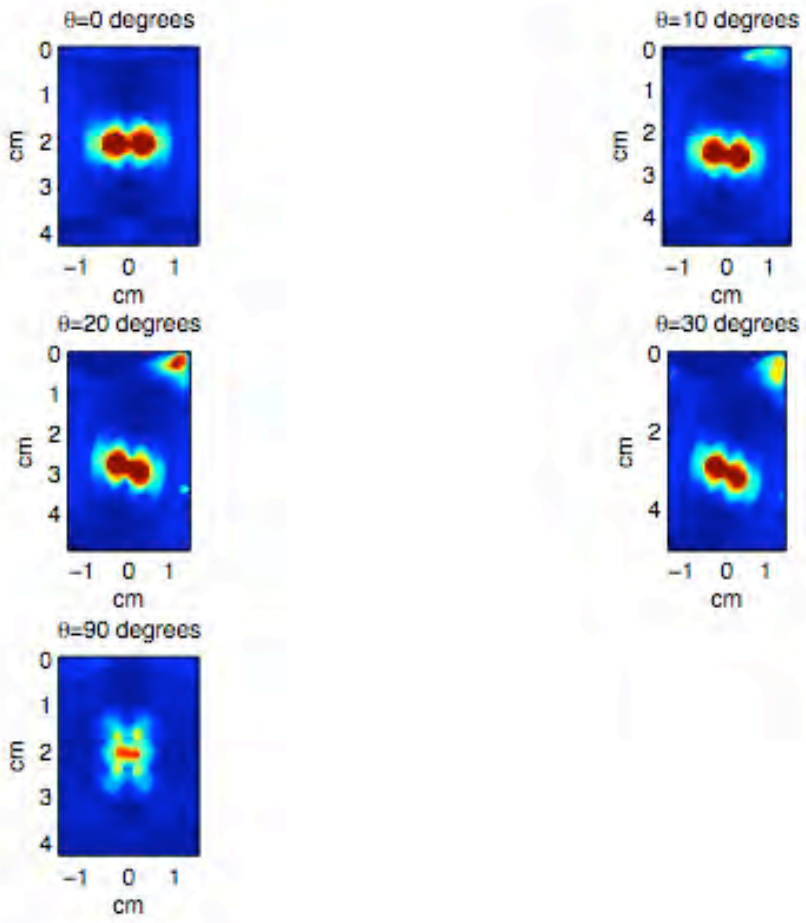

Figure 2. Motion amplitude estimates of seeds detected from simulated ultrasound echoes. Finite element simulations of seed and tissue motion in response to a sinusoidally varing magnetically induced force were used to displace scatterers in the ultrasound imaging model. The scatterers were rotated to orientations of 0, 10, 20, 30, and 90 degrees. In all cases, and in contrast with the B-mode images of Figure 1, the seed remains visible. Further, there is no speckle artifact in the motion estimate images to obscure the seeds.

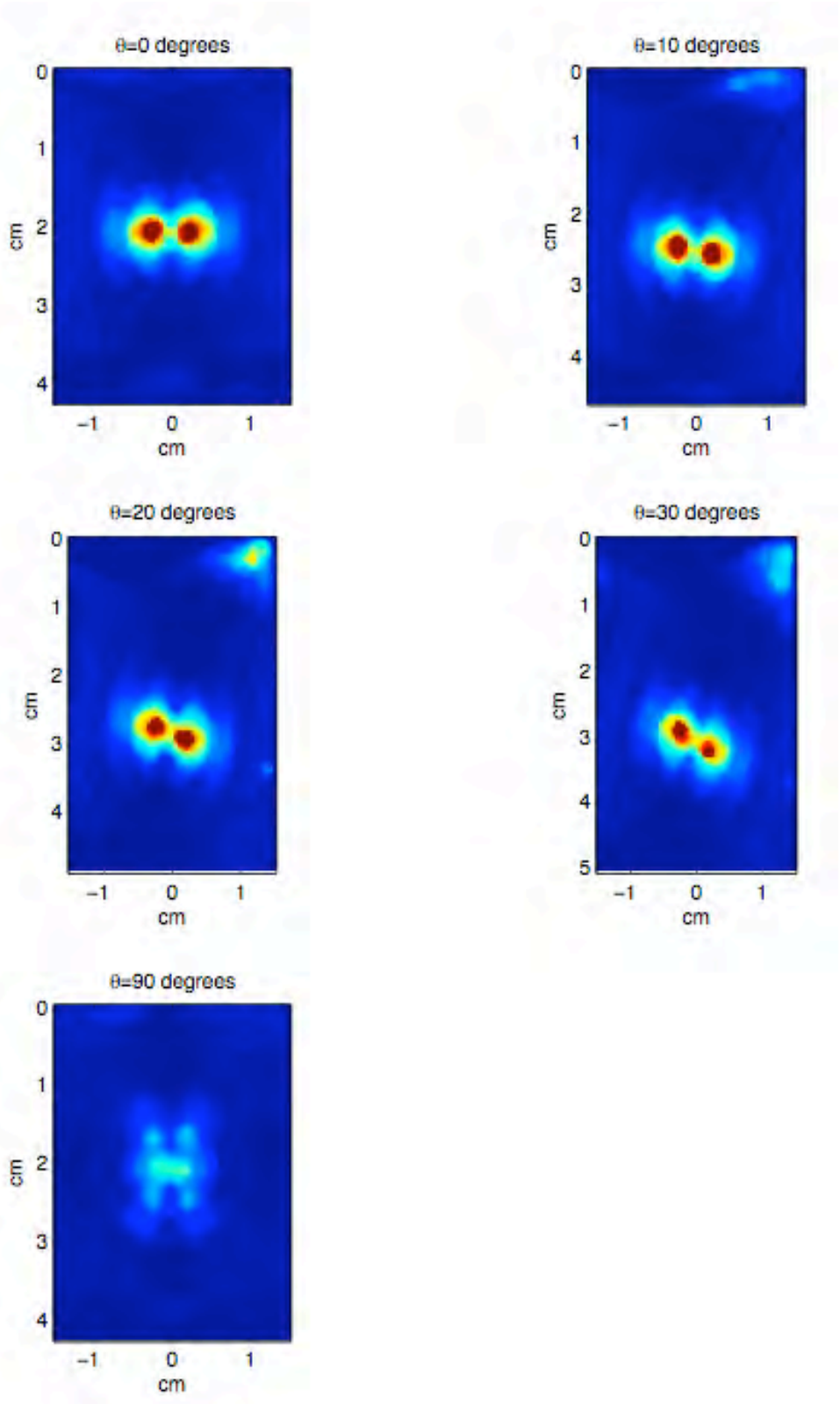

Figure 3. Motion estimate images of figure 2 presented with an expanded dynamic range. Here it is seen that the seed is still visible in all images, and that the seed location may be determined with greater precision than indicated in figure 2, with its saturated response.

(a)

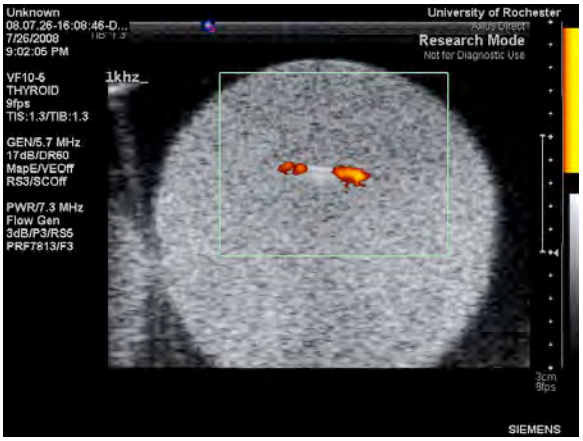

(b)

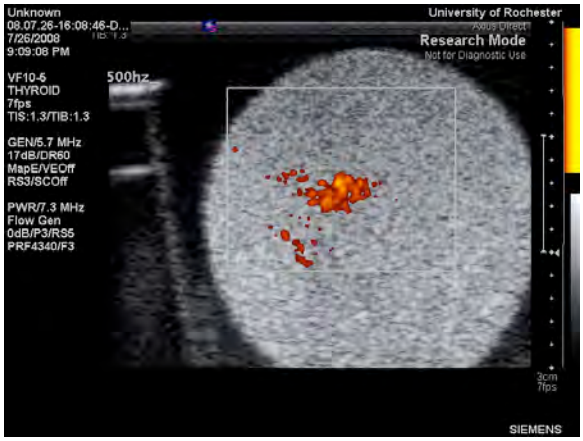

(c)

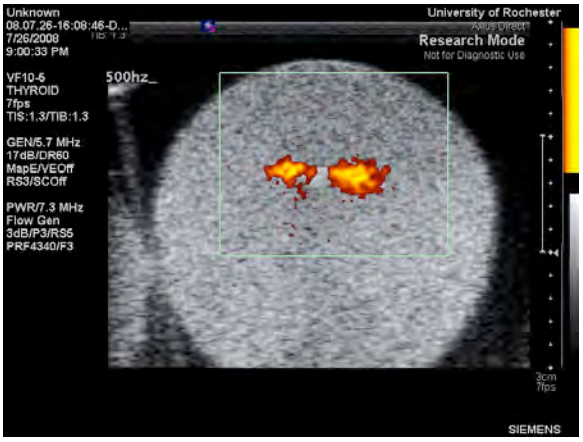

(d)

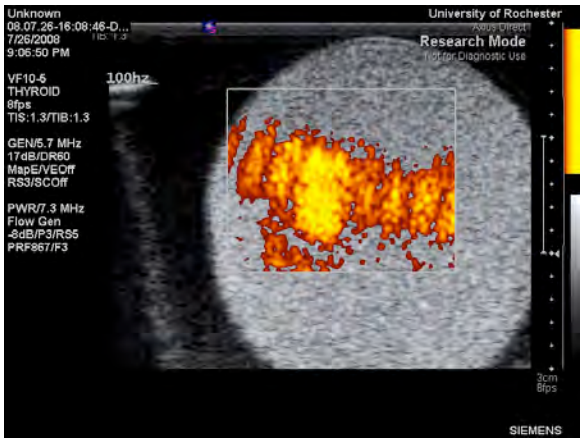

(e)

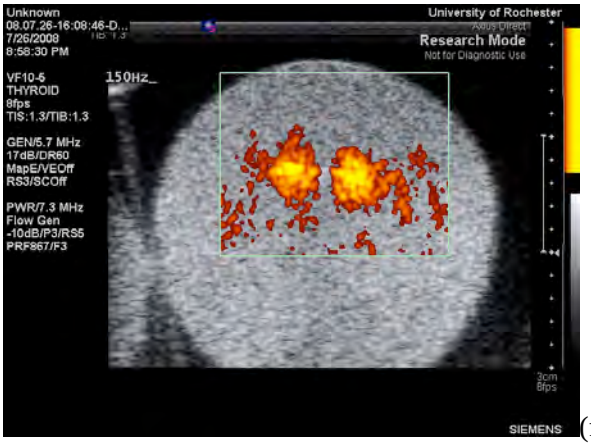

(f)

Figure 4. In vitro images of a seed in a tissue-mimicking phantom obtained using Power Doppler imaging. Seed orientation is 90 degrees (perpendicular to the transducer face) in (a,c,e) and 0 degrees (parallel to the transducer face) in (b,d,f). The seed is visible in both orientations, though it can be seen to be invisible in the 90 degree orientation in the B-scan (e.g. figure 4a) . Drive frequencies of 1000, 500, and 100Hz were used for the top, middle and bottom rows, respectively. The increased resolution available with higher drive frequency, and the larger area of induced motion at lower frequency, are evident.

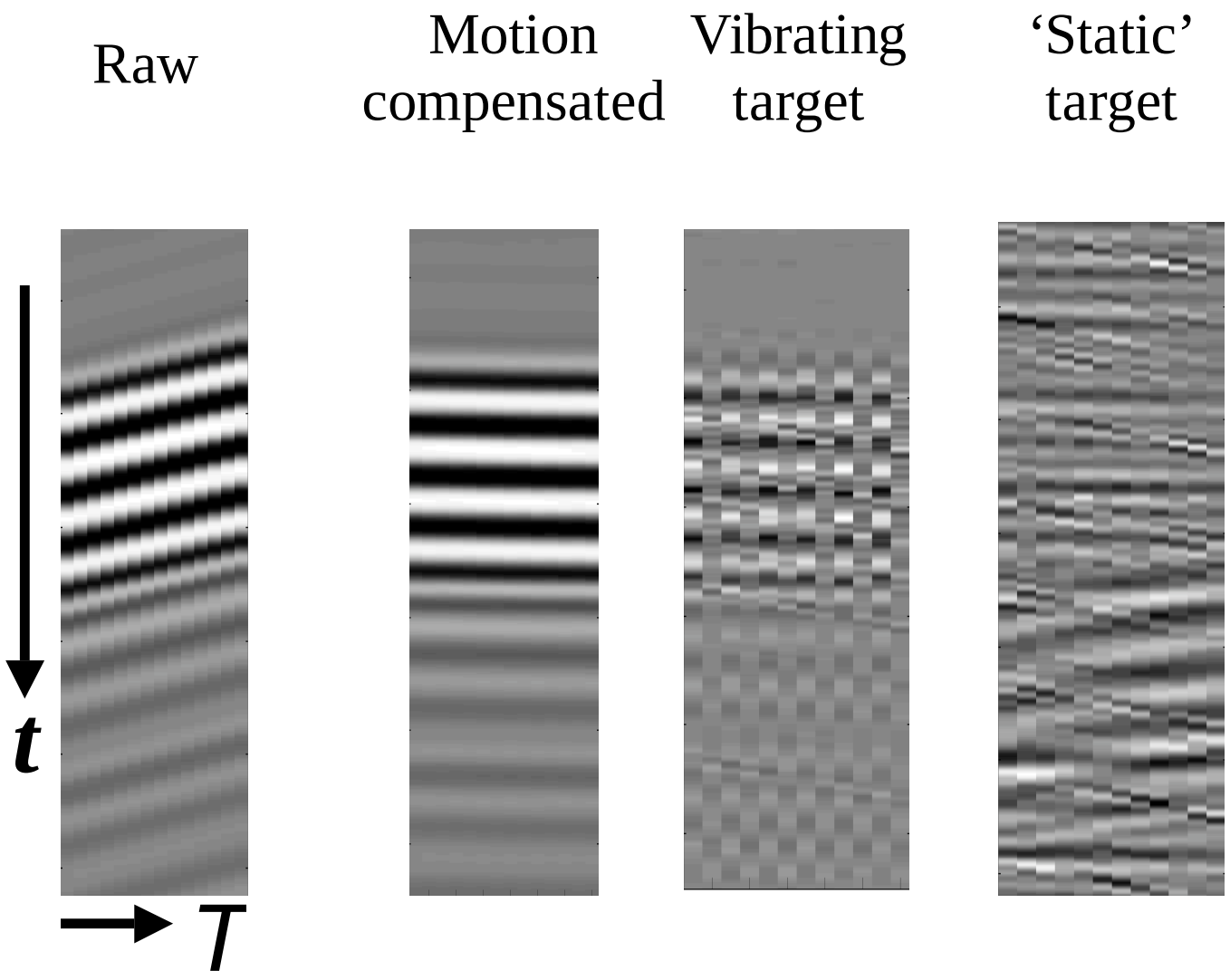

Figure 5. Steps in the clutter suppression algorithm. Raw Doppler data (a) is analyzed to determine a best-fit constant velocity estimate. The motion due to this constant velocity, assumed to be physiological or transducer motion, is subtracted from the Doppler ensemble by time shifting each echo (b). For a vibrating target (c), the vibration signal remains unaltered, while the static target (d) shows only noise. Stationary clutter suppression has been applied to (c) and (d).